Adhesion signaling in mammary gland development, tumorgenesis and progression

Miltenburg, M.H.A.M.

Chapter 5

Annexin A1 Regulates TGF-β-signaling and Promotes Metastasis Formation of Basal-Like Breast Cancer Cells

Martine HAM van Miltenburg*, Marjo de Graauw*, Marjanka K Schmidt, Chantal Pont, Reshma Lalai, Joelle Kartopawiro, Evangelia Pardali, Sylvia Le Dévédec, Vincent TBHM Smit, Annemieke van der Wal, Laura J Van't Veer,Anne-Marie Cleton-Jansen, Peter ten Dijke and Bob van de Water.

Accepted for publication in Proc. Natl. Acad. Sci.

Annexin A1 Regulates TGF-β-signaling and Promotes Metastasis Formation of Basal-Like Breast Cancer Cells

Martine HAM van Miltenburg[1,*], Marjo de Graauw[1,*], Marjanka K Schmidt[2], Chantal Pont[1], Reshma Lalai[1], Joelle Kartopawiro[1], Evangelia Pardali[4], Sylvia Le Dévédec[1], Vincent TBHM Smit[3], Annemieke van der Wal[3], Laura J Van't Veer[2], Anne-Marie Cleton-Jansen[3], Peter ten Dijke[4] and Bob van de Water[1]

[1]Division of Toxicology, Leiden/Amsterdam Center for Drug Research, Leiden University, Einsteinweg 55, P.O. Box 9502, 2300 RA Leiden, The Netherlands, [2]Department of Pathology, Netherlands Cancer Institute-Antoni van Leeuwenhoek Hospital, Amsterdam, The Netherlands, and [3]Department of Pathology, Leiden University Medical Centre, Leiden, The Netherlands
[4]Department of Molecular Cell Biology and Centre for Biomedical Genetics, LUMC, Leiden, The Netherlands

*These authors contributed equally to the manuscript

Abstract

Annexin A1 (AnxA1) is a candidate regulator of the epithelial- to mesenchymal (EMT)-like phenotypic switch, a pivotal event in breast cancer progression. We show here that, AnxA1 expression is associated with a highly invasive basal-like breast cancer subtype both in a panel of human breast cancer cell lines as in breast cancer patients, and that AnxA1 is functionally related to breast cancer progression. AnxA1 knock-down in invasive basal-like breast cancer cells reduced the number of spontaneous lung metastasis, while additional expression of AnxA1 enhanced metastatic spread. AnxA1 promotes metastasis formation by enhancing TGFβ/Smad signaling and actin reorganization, which facilitates an EMT-like switch, thereby allowing efficient cell migration and invasion of metastatic breast cancer cells.

Introduction

Annexin A1 (AnxA1) belongs to the family of calcium/phospholipid-binding and actin regulatory proteins (1). Using proteomic analysis we have previously identified AnxA1 as well as its family member AnxA2 as candidate regulators of oncogene-induced cell morphology switch (2). During such a switch tumor cells change from an epithelial- to a more migratory, mesenchymal-like phenotype. This enables them to increase their motility and invasiveness, allowing metastasis and progression of breast cancer (3). Despite the identification of AnxA1 as one of several cellular proteins that is differentially expressed during the progression of tumors to more malignant states (4), a functional role for AnxA1 in breast cancer progression and metastasis is lacking (5, 6). Therefore we set-out to study AnxA1 expression in different breast cancer cell subtypes and its role and mechanism in the control of breast cancer progression and metastasis formation.

Several different subtypes of breast carcinomas can be identified based on gene expression profiling studies (e.g. luminal A, luminal B, normal breast-like, ErbB2-positive and basal-like) (7, 8). These subtypes differ in their morphology, clinical course and response to therapy. For example, while the luminal subtype is characterized by its mild invasive capacity and relatively good clinical outcome, the basal-like subtype is characterized by enhanced invasiveness and formation of distant metastasis and thereby a poor clinical outcome (7, 9). The enhanced metastatic capacity of basal-like breast cancer (BLBC) is associated with their migratory, mesenchymal-like phenotype (10).

Here we show that high AnxA1 expression is associated with the BLBC subtype in a panel of breast cancer cell lines. Depletion of AnxA1 in BLBC cells resulted in reversal of their migratory, mesenchymal-like phenotype, which was associated with actin reorganization, decreased TGFβ/Smad signaling, and a reduction in the number of spontaneous lung metastasis *in vivo*. Moreover, using tissue micro arrays we show that AnxA1 clearly discriminates BLBC patients from other breast cancer patients.

Results

High AnxA1 expression in BLBC is associated with their mesenchymal-like phenotype

To establish the relationship between AnxA1 expression and breast cancer cell phenotype, a panel of human breast cancer cell lines was screened for AnxA1 expression. AnxA1 was highly expressed in cells that were characterized as mesenchymal-like (11) and classified as $CK5^{+}/ER^{-}$ basal-like breast cancer cells (BLBC) (12, 13) (Fig. 1A and 1B). In contrast, $CK5^{-}/ER^{+}$ luminal-like breast cancer cells almost completely lacked AnxA1 (Fig. 1A and 1B).

To verify whether AnxA1 regulates the migratory, mesenchymal-like phenotype of BLBC cells, AnxA1 was depleted in a selection of these cells using either transient siRNA- or stable lentiviral shRNA-mediated knock-down.

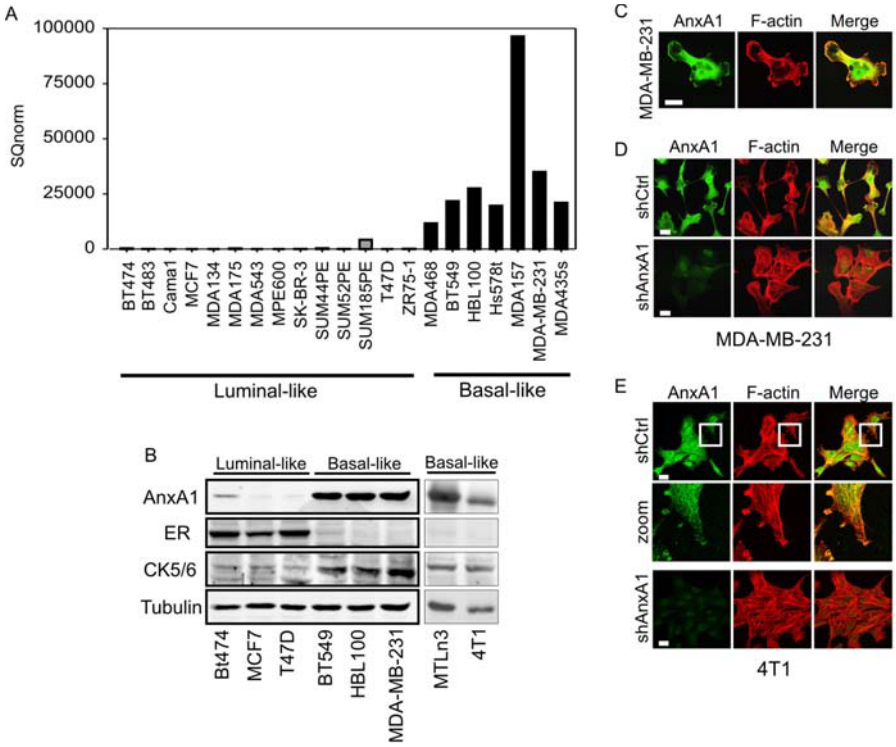

Fig. 1. *AnxA1 expression in BLBC is associated with their migratory phenotype*
A panel of human breast cancer cell lines was analyzed for AnxA1 mRNA levels (A). Western blot analysis of AnxA1 protein levels in luminal-like (BT474, MCF7, T47D) versus basal-like (HBL100, BT549, MDA-MB-231) human breast cancer cell lines and basal-like mouse 4T1 and rat MTLn3 cells (B). AnxA1 localization was determined in MDA-MB-231 cells by staining for AnxA1 (green) and actin (red) (C). Knock-down in MDA-MB-231 and 4T1 cells was established using lenti-viral shRNA specific for turbo-GFP (Control shRNA) and AnxA1 (AnxA1 shRNA1) (D-E). Cells were plated on collagen and subsequently fixated and stained for AnxA1 and F-actin (rhodamin-phalloidin). Bars, 20 μm. Data are representative of three independent experiments.

In control cells, AnxA1 is localized at the plasma membrane site, in the actin-rich membrane ruffles (MDA-MB-231) and migratory tips (4T1), which are required for migration, invasion and metastasis (Fig. 1C-E). In all selected BLBC cells, AnxA1 knock-down resulted in a morphological switch from a migratory, mesenchymal-like phenotype to a resting, epithelial-like phenotype (Fig. 1C-E and S1A-D). This reversal of the migratory phenotype was associated with a clear rearrangement of the actin cytoskeletal network; actin-rich ruffles were lost and

long F-actin stress fibers were obtained (Fig. 1D-E). Moreover, AnxA1 knock-down induced the formation of β-catenin-containing cell-cell junctions in all cells, which were most clearly visible in the highly motile MTLn3 cells (Fig. S1C-D). In addition, AnxA1 knock-down significantly reduced the migration distance and random cell migration speed of siAnxA1 MTLn3 cells (Suppl. Fig. S1E-G and movies 1-3). The AnxA1 knock-down-induced epithelial-like morphology of MTLn3 cells was rescued by ectopic expression of AnxA1 (Fig. S1C-D). These combined data demonstrate that AnxA1 is involved in an EMT-like switch, facilitating cell migration *in vitro.*

Knock-down of AnxA1in BLBC cells impairs TGF-signaling

The switch from an epithelial to a mesenchymal-like phenotype is, amongst other pathways, regulated by TGFβ signaling (14). Since AnxA1 knock-down induces a morphological switch from a mesenchymal- to an epithelial-like phenotype in different BLBC cells, we determined its influence on TGFβ signaling. TGFβ induces clustering of TGFβRI and II and subsequently phosphorylation of Smad2. AnxA1 knock-down in MDA-MB-231 cells impaired Smad2 phosphorylation in response to TGFβ exposure (Fig. 2A-B). Smad2 phosphorylation is a trigger for Smad2 to form a complex with Smad4, resulting in nuclear translocation of the Smad2/Smad4 complex and subsequent gene transcription. AnxA1 knock-down MDA-MB-231 cells exposed to TGF show less nuclear translocation of Smad4 (Fig. 2C-D). In addition, knock-down of AnxA1 in MDA-MB-231, BT549 and MTLn3 cells, resulted in reduced activity of TGFβ/Smad3/Smad4-driven $(CAGA)_{12}$-luciferase transcriptional reporter activity (Fig. 2E-G), indicating that AnxA1 is also involved in the regulation of TGFβ/Smad3 response. Furthermore, the TGFβ-type I receptor inhibitor SB-431542 (15) reduced $(CAGA)_{12}$-luciferase activity in MTLn3 cells both in the absence and presence of TGFβ (Fig. S2A), and reversed the mesenchymal-like phenotype (Fig. S2B) similar to the morphological switch observed in AnxA1 knock-down cells (Fig. S1C-D). Moreover, TGFβ alone enhanced cell scattering (Fig. S2B). Altogether, the data suggest that AnxA1 is involved in TGFβ-induced EMT-like switch.

Expression of AnxA1 induces an EMT-like switch by activation of the TGFβ-pathway

Next we considered whether AnxA1 expression in a typical luminal-like breast cancer cell line that has low AnxA1 expression, would induce a scattered phenotype. Indeed, AnxA1 expression in luminal-like MCF7 cells resulted in increased cell scattering (Fig. 3A-B), which was associated with a disruption of F-actin stress fibers, an increase in actin-rich ruffles and a decrease in β-catenin-containing cell-cell junctions (Fig. 3A-B and S2E). MCF7 cells expressing AnxA1 showed increased TGFβ-induced Smad3/Smad4 transcriptional reporter activity explaining the increase in cell scattering (Fig. 3C).

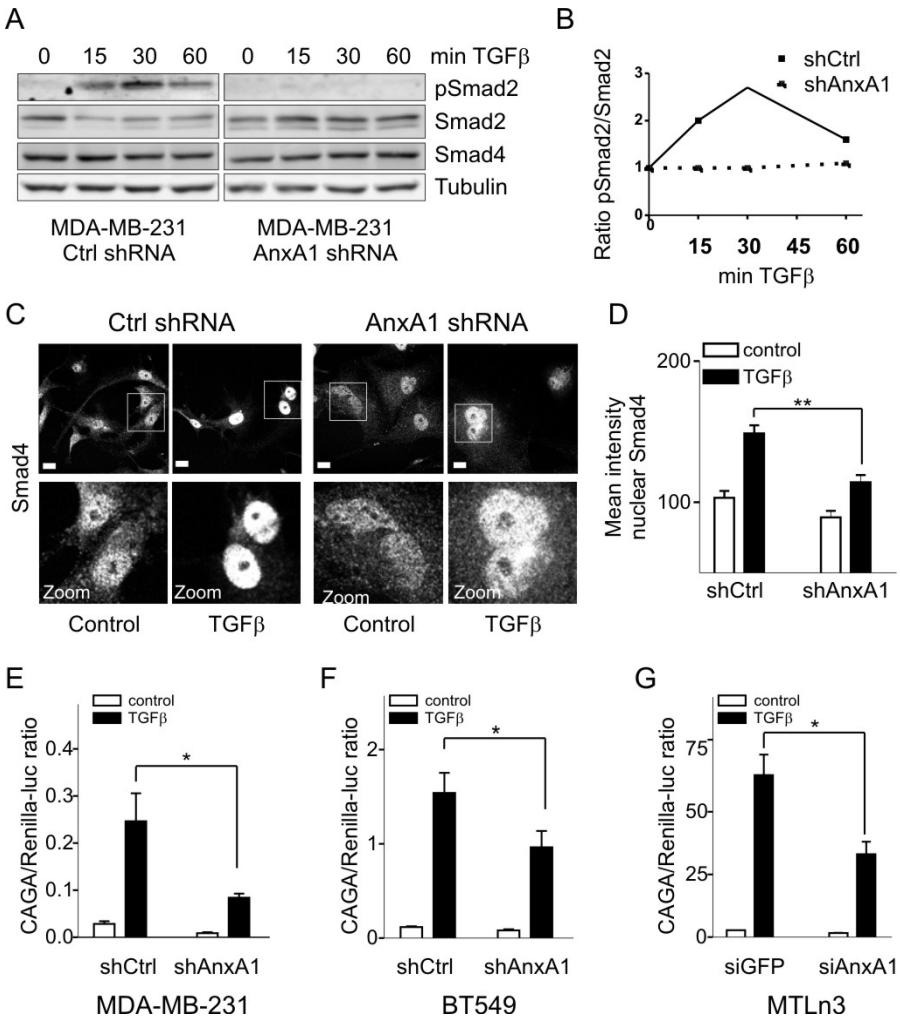

Fig. 2. *Knock-down of AnxA1in basal-like breast cancer cells impairs TGF-signaling*
Stable MDA-MB-231 knock-down cells were exposed to TGFβ 1 ng/ml) for indicated time periods. Phosphorylation of Smad2, Smad2 and Smad4 expression was determined by Western blotting (A). Quantification of Smad2 phosphorylation (B). Translocation of Smad4 was determined by Smad4 staining of MDA-MB-231 cells exposed to TGFβ1 for 30 min (C) and quantification of nuclear intensity (D). TGFβ1-induced transcription was determined by transient transfection of $(CAGA)_{12}$-luciferase in AnxA1 depleted MDA-MB-231 (E), BT549 (F) and MTLn3 cells (G). After transfection cells were exposed to TGFβ1 (0.5 ng/ml) for 24 h.

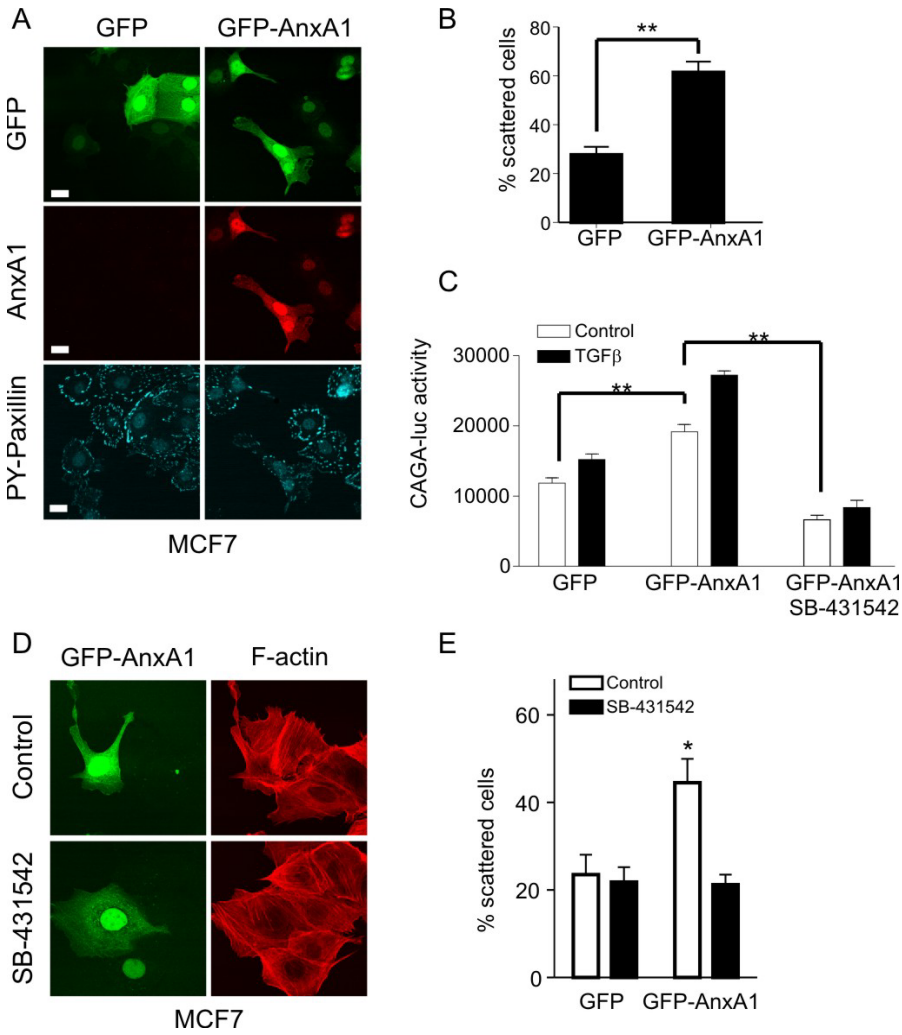

Fig. 3. *AnxA1 induced cell scattering in luminal-like MCF7 cells through TGFβ pathway activation.* MCF7 cells were transfected with GFP or GFP-AnxA1. Cells were plated on collagen for 24 hrs and subsequently fixated and stained for AnxA1. Cells were co-stained with phosphoY118-paxillin to visualize all cells within the frame (A). The number of scattered cells was determined for the GFP positive cells (B). Co-transfection of $(CAGA)_{12}$-luc and GFP-AnxA1 was performed and cells were exposed to TGFβ and/or SB-431542 and thereafter luciferase activity was measured (C). MCF7 cells expressing GFP-AnxA1 were exposed to SB-431542 and stained for F-actin (D). Cell scattering induced by AnxA1 expression was reduced by SB-431542 (E). Bars, 20 μm. Data are representative of three independent experiments. * $p<0.05$, ** $p<0.01$.

Increased TGFβ-induced Smad3/Smad4 transcriptional reporter activity was also observed in epithelial-like cell lines BT474 and T47D cells (Fig. S2C and S2D, respectively) The AnxA1-induced increase in Smad3/Smad4 transcriptional response was inhibited by the TGFβ type I receptor inhibitor SB-431542, suggesting that AnxA1 might affect an autocrine signaling loop of TGFβ–induced receptor activation (Fig. 3C). This was supported by the observation that AnxA1-expressing MCF7 cells exposed to the SB-431542 showed a morphological change from a mesenchymal-like to an epithelial phenotype (Fig. 3D-E). Overall, our data strongly support the importance of AnxA1 in the regulation of a morphological switch from a resting epithelial-like to a migratory phenotype through regulation of the TGFβ/Smad pathway.

Knock-down of AnxA1 decreases the metastatic potential of highly aggressive 4T1 cells

Next we determined whether AnxA1 depletion from highly invasive breast cancer cells can reduce metastasis formation *in vivo*. Therefore, the well characterized invasive breast cancer cell line 4T1 was used, which is able to spontaneously metastasize from a primary tumor *in vivo* (16). To establish AnxA1 depletion in 4T1 cells two independent lenti-viral shRNA were used (Fig. 4A). The control cell line expresses a shRNA sequence against turbo-GFP. Cells were injected into the mammary fat pads of 12 week old Rag2 $^{-/-}$ /γc $^{-/-}$ mice. Knock-down of AnxA1 had no effect on primary tumour growth (Fig. 4B and S3B). Mice were sacrificed at day 22, and histological evaluation of the primary tumor confirmed decreased expression of AnxA1 in tumors derived from AnxA1 shRNA cells (Fig. S3A). Lungs of animals injected with control 4T1 contained over 130 surface metastases (Fig. 4C-E), while animals injected with either AnxA1 knock-down 4T1 contained on average about 30 surface metastases (Fig. 4C-E). In line with our findings in Rag2 $^{-/-}$ /γc $^{-/-}$ mice, AnxA1 knock-down did not affect primary tumour growth, but significantly reduced the number of lung metastases in syngenic Balb/C mice (Fig. S3B-C). In addition, metastasis formation of AnxA1 knock-down MTLn3 cells was markedly reduced (Fig. S3D-E).

The reduction in metastasis formation by AnxA1 depletion was associated with reduced TGFβ/Smad signaling. Smad2 phosphorylation in primary tumors was reduced as well as the nuclear levels of Smad4 (Fig 4F-G, respectively). Our *in vivo* data indicate that the morphological changes induced by AnxA1 knock-down are linked to a decrease in breast cancer progression via the effect on TGFβ/Smad signaling.

AnxA1 distinguishes basal-like breast cancer patients from others.

To verify our finding that AnxA1 is expressed in a specific subset of breast cancer cells, human tissue microarrays (TMA) containing tissues of 452 breast cancer patients were analyzed. In contrast to normal breast tissue where AnxA1 is

localized in both the luminal and myoepithelial cell layer (Fig. 5A), in pre-malignant breast tissue AnxA1 was mainly expressed in the myoepithelial cell layer, where it localized both in the cytosol as well as the nucleus (Fig. 5B (zoom a)). In breast cancers, the majority of the tumor tissue showed negative (Fig. 5B (a,b) n = 323) or low expression (n = 85) of AnxA1, while approximately 10% showed high expression of AnxA1 (Fig. 5B (c,d) n = 44). The AnxA1 negative/low cases included both ductal carcinoma in situ (DCIS) as well as invasive ductal carcinoma (IDC), while AnxA1 positive tumors included mainly IDC (Fig. 5B and S4). Further analysis revealed that AnxA1 expression correlated with high pathologic tumor grade ($P<0.001$ (Fig. S5A, Supplemental table 1A).

In addition to AnxA1, TMAs were stained and scored for AnxA2 and 6 markers currently used for the identification of specific subgroups of breast tumors (e.g. HER2, the hormonal receptors ER and PR, basal and luminal cytokeratins CK5 and CK8 respectively, and p53). Statistical analysis of the expression data confirmed an overall significant correlation between AnxA1 expression and proteins associated with BLBC (e.g. $p53^{high}$, $CK5^{high}$, ER^{low}, $CK8^{low}$) (Fig. S5B-E, Supplemental table 1B-E), suggesting that AnxA1 is also predictive for BLBC in breast cancer patients.

Unsupervised hierarchical clustering of the protein expression data subdivided all breast cancers into four clusters: a small undefined $CK5^{+}/8^{+}/ER^{+}$ group (1; ~5%), ER^{+}/luminal-like (2; ~60%), HER2-positive (3; ~20%), and triple negative ($ER^{-}/PR^{-}/HER2^{-}$) (4; ~15%) (Fig. 5C and S5). AnxA1 was almost exclusively expressed in the small $CK5^{+}/8^{+}/ER^{+}$ subgroup (1) and triple negative breast cancer subgroup (4), while its close family member AnxA2 was expressed in all four clusters. Moreover, a clear correlation was found between p53 and AnxA1 expression within the triple negative subgroup. Although, triple negative breast cancers are described as a heterogeneous group of cancers, the majority displays a basal-like phenotype (17). CK5 expression, either in association with lack of ER/PR/HER2 or alone (17, 18), is often used to define the poor prognosis basal-like breast cancer (BLBC) subtype. Our cluster analysis revealed that AnxA1 clusters directly with CK5, a marker for the BLBC subtype (Fig. 5C).

Fig. 4 (right page). *Knock-down of AnxA1 decreases the metastatic potential of highly invasive 4T1 cells via decreased TGFβ signaling.*

Mouse breast cancer 4T1 cells were transduced with lenti-viral shRNA specific for turbo-GFP (control shRNA) and two sequences for AnxA1 (AnxA1 shRNA1 and 2). AnxA1 knock-down was determined by Western blot analysis (A). AnxA2 levels were included in the analysis to show specificity of the shRNAs. Equal loading was confirmed by tubulin staining. AnxA1 shRNA1 (n=6), AnxA1 shRNA2 (n=6) and control shRNA (n=7) 4T1 cells were injected into the mammary fat pad of 12 week old $Rag2^{-/-}/\gamma c^{-/-}$ mice. Tumour volume was determined as described in Material and Methods (B). At 22 days after injection the mice were sacrificed and lungs were isolated. Lung sections were stained for haematoxylin/eosin to visualize lung metastases (C). Lungs were inoculated with ink as described under materials and methods (D) and surface metastases were quantified (E). $p < 0.001$ (***). Primary tumors were stained for p-Smad2 and Smad4 using Nova-Red staining and quantified for equal expression of Smad2 and Smad4 using Western blotting (F-G). * $p<0.05$, ** $p<0.01$.

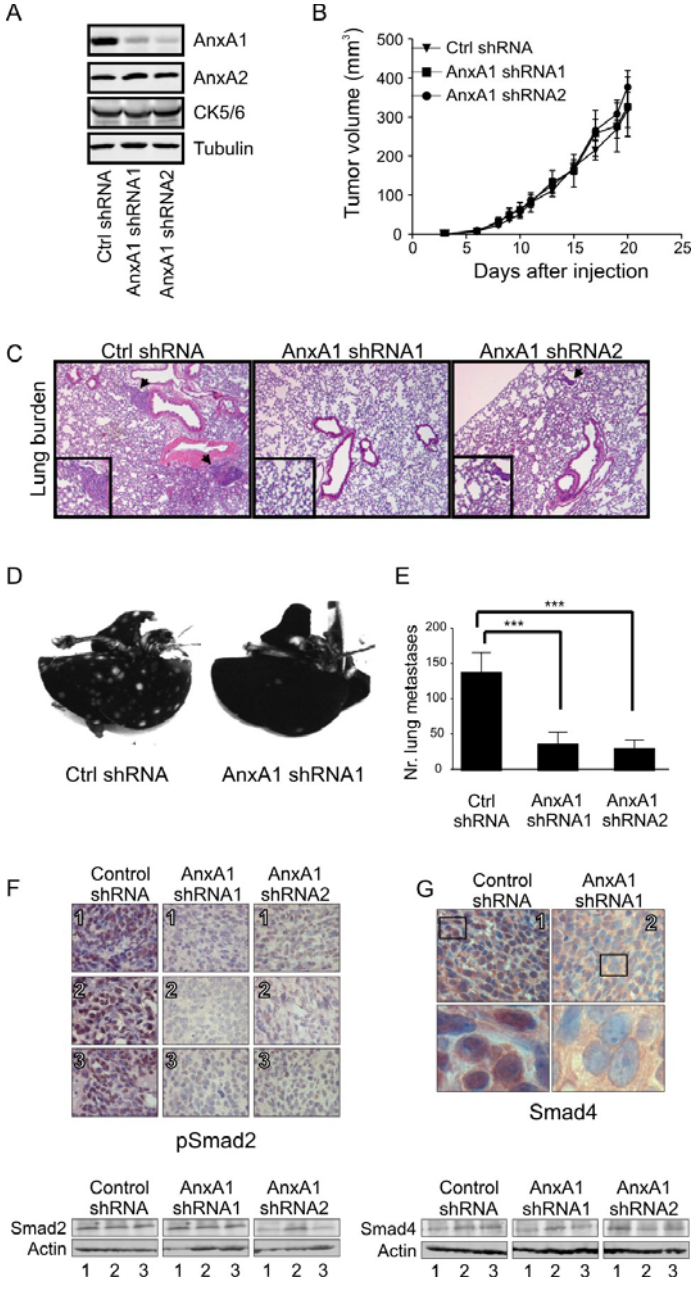
A
AnxA1
AnxA2
CK5/6
Tubulin
Ctrl shRNA
AnxA1 shRNA1
AnxA1 shRNA2
B
Tumor volume (mm3)
Ctrl shRNA
AnxA1 shRNA1
AnxA1 shRNA2
Days after injection
C
Ctrl shRNA
AnxA1 shRNA1
AnxA1 shRNA2
Lung burden
D
Ctrl shRNA
AnxA1 shRNA1
E
Nr. lung metastases
***
***
Ctrl shRNA
AnxA1 shRNA1
AnxA1 shRNA2
F
Control shRNA
AnxA1 shRNA1
AnxA1 shRNA2
pSmad2
Smad2
Actin
G
Control shRNA
AnxA1 shRNA1
Smad4
Smad4
Actin

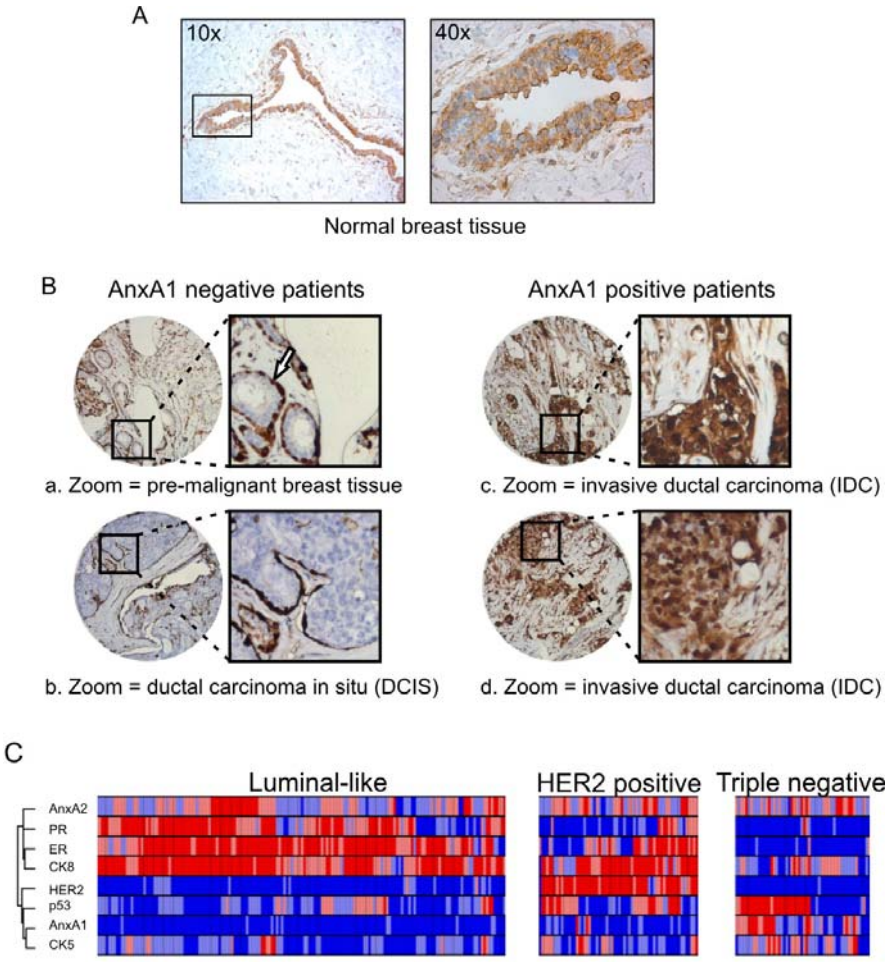

Fig. 5. AnxA1 discriminates basal-like breast cancers from other subtypes
Normal breast tissue was stained for AnxA1 (A). Human breast cancer tissues (TMA of 452 patients) were screened for AnxA1, AnxA2, and 6 clinical markers CK5, CK8, ER, PR, HER2 and p53. Representative images are shown for pre-malignant breast tissue (a, note the AnxA1 positive myoepithelial cells pointed by an arrow), AnxA1 negative ductal carcinoma in situ (DCIS) (b), and AnxA1 positive, invasive ductal carcinoma (IDC) (c & d) (B). Only those breast carcinomas where staining for all the 8 immunohistochemical markers was successful (n=295) were included for hierarchical unsupervised cluster analysis (B) and tumors were divided luminal-like, HER2+ and triple negative groups (C).

Moreover, our unsupervised hierarchical clustering showed that CK5 is not solely expressed in the triple negative group, but also in the luminal-like and $HER2^+$ tumor samples. In contrast, AnxA1 is almost exclusively expressed in the triple negative subgroup (marker prediction of a tumor to be in the triple negative subgroup versus any other subgroup (Odd Ratios (95% confidence interval)): CK5 2.2 (1.2-4.2), p=0.01 and AnxA1 10.5 (4.9-22.2), p<0.0001). Due to the small number of AnxA1 positive patients, we were unable to significantly correlate AnxA1 protein expression to recurrence and relapse-free survival, yet a clear trend was observed between AnxA1 protein expression and recurrence. In addition, within the specific gene signature for poor prognosis defined by van 't Veer *et al.* (19), AnxA1 gene expression was significantly higher in basal-like than in the other tumor subtypes (p<0.001) (Supplemental table S2). Altogether our data shows that AnxA1 is associated with the BLBC-subtype and functionally involved in basal-like breast cancer progression and metastasis formation by regulating TGFβ-signaling and actin cytoskeletal reorganization.

Discussion

Basal-like breast cancers (BLBCs) represent less than 10% of all breast cancers and show enhanced invasiveness and metastatic potential (9). Given the poor disease prognosis associated with BLBC, improving methods to accurately identify BLBC in the clinic as well as better mechanistic understanding of the molecular programs that define the metastatic potential are essential. Our data demonstrated that BLBCs express high levels of AnxA1 and that AnxA1 is important for their capacity to metastasize since it facilitates a migratory phenotype.

Depletion of AnxA1 in a panel of BLBC cells resulted in reversal of their migratory phenotype and inhibition of lung metastasis formation. We show that AnxA1 expression controls the aggressive behavior of BLBC cells via a TGFβ-mediated EMT-like switch, thereby allowing a migratory phenotype of breast cancer cells and metastasis formation. AnxA1 knock-down suppressed TGFβ-induced Smad2 phosphorylation, Smad4 nuclear translocation and Smad3/Smad4 driven transcriptional reporter activity. Moreover, primary tumors with AnxA1 knock-down had a reduced Smad2 phosphorylation and Smad4 nuclear localization. A biological role of AnxA1 is not restricted to BLBC-like tumor cells. Despite the fact that luminal-like breast tumor cells do not express AnxA1, ectopic expression of AnxA1 in luminal-like MCF7 cells resulted in a clear EMT-like switch. Moreover, enhanced TGFβ signaling now occurred in these cells. Therefore it is likely that such a role of AnxA1 is also relevant in other aggressive tumor cell types. Our data on the role of TGFβ in the metastasis formation are in conjunction with the study of Deckers *et al.* that demonstrated that TGF signaling via Smad4 is required for TGF-induced EMT and bone metastasis formation of NMuMG and MDA-MB-231 cells respectively (20). Moreover,

TGFβ in the breast tumor microenvironment was shown to prime cancer cells for metastasis to the lungs (21) and TGFβ antagonists reverse the migratory phenotype that is characteristic of BLBC cells, thereby affecting the progression of BLBC (22). We anticipate that AnxA1 is a central player in TGFβ-signaling dependent cancer progression.

Members of the annexin family have been shown to be involved in endocytosis (23-27). Although AnxA1 was enriched in membrane fractions containing early endosomes (28), it remains unclear how AnxA1 is involved in endocytosis, and in particular endocytosis of TGFβ-receptors. Inhibition of TGFβ receptor endocytosis results in decreased Smad2 phosphorylation and Smad-mediated gene transcription (29-31). We propose that AnxA1 may influence TGFβ signaling by interfering with TGFβ-receptor endocytosis.

In addition to its direct effect on endocytosis, AnxA1 may influence internalization of TGFβ-receptors indirectly via regulation of the actin cytoskeleton like has been described for AnxA2 (27). Decreased actin cytoskeletal dynamics as observed in our AnxA1 knock-down cells might stiffen the cell membrane thereby impeding TGFβ-receptor internalization. Compared to other actin-regulatory proteins, AnxA1 has the unique property to bind both phospholipids at the plasma-membrane as well as F-actin, thereby stabilizing and/or regulating membrane-actin interactions (32).

To define BLBCs in the clinic, pathologists often use immuno-histochemical staining of the classical marker CK5. However, we and others show that CK5 is also expressed in luminal-like and HER2 breast cancers suggesting that the sole reliance on CK5 could result in false positive characterization (Fig. 5) (33). Our tissue micro array (TMA) data analysis revealed a significant correlation between high AnxA1 protein expression and the BLBC subtype without any high expression levels in the luminal-like or HER2 breast cancers (Fig. 5). Moreover, AnxA1 gene expression was significantly higher in basal-like than in the other tumor subtypes in the poor prognosis gene signature of van ‘t Veer et al (19) ($p<0.001$) (table S2) and AnxA1 was found to be over-expressed in two gene signatures described to distinguish basal-like breast cancer from other subtypes (7, 34). Therefore, we propose AnxA1 as an additional marker to improve diagnostics to better discriminate basal-like breast cancers from other subtypes in the clinic. Currently we are collecting patient material and data for a larger cohort study performed by several independent pathologists (in total over 2000 patients), which will validate the potential of AnxA1 as an official marker for improved identification of the highly aggressive basal-like breast cancer subtype and its association with a poor prognosis.

Taken together our data show that AnxA1 is functionally involved in BLBC progression and metastasis formation and is able to regulate TGFβ-signaling and actin cytoskeletal reorganization. We propose AnxA1 as an

additional marker to improve diagnostics to better discriminate basal-like breast cancers from other subtypes in the clinic.

Materials and Methods

Cell line maintenance and treatments. The breast cancer cell lines used for real-time PCR analysis in this study were cultured and characterized for morphology (e.g. epithelial vs mesenchymal) and E-cadherin promoter methylation as described (11). MTLn3 rat mammary adenocarcinoma cells (35) were cultured as described previously (36). The 4T1 mouse breast cancer cell line was obtained from American Type Culture Collection (ATCC) (CRL-2539) and cultured in RPMI-1640 Medium (Gibco) supplemented with 10% fetal bovine serum.

RNA isolation and real-time PCR. Cell culture of the panel of breast cancer cell lines described in Fig. 1A, RNA isolation and RT-PCR was performed as previously described (11).

Expression and knock-down of AnxA1. For preparation of stable shRNA cell lines, 4T1, MDA-MB-231 and BT549 cells were transduced using lenti-viral shRNA vectors (Sigma-Aldrich, kindly provided by dr. Hoeben, LUMC). See SI methods for sequences. Cells were selected using puromycin. For transient knock-down of AnxA1 Dharmacon *Smartpool*™ siRNA's against GFP (control) or AnxA1 (rat and human) were used. Transfections were performed according to the manufacturer's protocol using Dharmafect reagent 2 (MTLn3) and 4 (MDA-MB-231, HBL-100) (Dharmacon®).

Live-cell imaging

For live-cell imaging of cell migration (siRNA transfected) MTLn3 cells were cultured on collagen coated 24 wells glass bottom plates (Sensoplate, Greiner Bio-One) for 24 h and after 2 h of serum starvation stimulated with EGF (60 ng/ml, Sigma) and/or TGFβ1 (1 ng/ml, R & D systems). Cells were visualized with time lapse microscopy for 300 min. Image acquisition was performed using a Nikon TE2000 combined with a Prior stage and controlled by NIS Element Software. Differential interference contrast (DIC) time-lapse videos were recorded using a charged coupled device (CCD) camera controlled by NIS Element Software. All images were processed and quantitative image analysis was performed using Image-Pro® Plus (Version 5.1; Media Cybernetics).

Animals

Female BALB/c mice aged between 10 and 12 weeks were purchased from Janvier (BALB/c j ce Rj); 12-week old Rag2 $^{-/-}$ γc $^{-/-}$ mice were obtained from in house breeding. Animals were housed in individually ventilated cages under sterile conditions. Housing and experiments were performed according to the

Dutch guidelines for the care and use of laboratory animals (UL-DEC-6117). Sterilised food and water were provided ad libitum.
At the indicated time points, animals were anesthetized with Nembutal and the primary tumor and lungs were excised. After the weight of the primary tumor was determined, the primary tumor and the left lung were divided into two pieces and either frozen in liquid nitrogen or fixated in 4% paraformaldehyde. The right lung was injected with ink solution and thereafter destained in water and fixated in Feketes [4.3% (v/v) acetic acid, 0.35% (v/v) formaldehyde in 70% ethanol].

In vivo tumor growth and metastasis formation. $1*10^5$ 4T1 tumor cells in 0.1 ml PBS were injected into the fat pad of 12 week old female Rag2 $^{-/-}$ $\gamma c^{-/-}$ or BALB/c mice. Size of the primary tumors was measured by using calipers. Horizontal (*h*) and vertical (*v*) diameters were determined and tumor volume (*V*) was calculated: $V = 4/3\pi(1/2[\sqrt{}(h \times v)]^3)$. Surface lung metastases were counted for each animal using ink injected lungs (n=5-7 per group). See SI methods for details on breeding and procedures. All animal experiments were approved by the local ethical committee.

Antibodies.
Anti-AnxA1 (Human) BD transduction laboratories (610066), anti-AnxA1 Zymed (71-3400), anti-AnxA2 BD transduction laboratories (610068), anti-ER Santa Cruz (Sc-543) and for TMA anti-ER Neomarkers, Labvision (MS-750), anti-paxillin^{Y118} Biosource (44-722), anti-Src Upstate biotechnology (05-184), anti-progesterone receptor PR-1 Immunologic, anti-p53 DAKO (M-7001), Her2/Neu Neomarkers, Labvision (MS-599), anti-Tubulin Sigma-Aldrich (T-9026), anti-Rhodamin-Phalloidin Molecular Probes (R415), anti-β-catenin BD transduction laboratories (C-19220), anti-CK5/6 DAKO (clone D5/16 B4), anti-CK5 Covance (PRB-160P), anti-CK8 Fitzgerald (rdi-pro61038), anti-Smad2 (ser465/467) Cell Signaling (#3108), anti-Smad2 (50), and anti-Smad4 Santa Cruz (sc-7966).

Immunofluorescence and image analysis
Cells were stained with specific antibodies recognizing for β-catenin, phospho-paxillin (pY118) overnight at 4 °C and subsequently incubated with Alexa-488 or Cy-3 conjugated secondary antibody (Molecular Probes) in combination with rhodamin-phalloidin (Molecular Probes) to label the F-actin cytoskeletal network. Microscopic analysis was performed using a Bio-Rad Radiance 2100 confocal laser scan microscope.

Immunohistochemistry. Tumors and lungs were embedded in paraffin and sectioned (4 µm) onto 3-aminopropyltriethoxysilane-coated slides. After deparaffinization the tumor and lung sections were stained for HE and lungs were examined for lung metastasis formation. Paraffin sections were deparaffinized,

followed by antigen retrieval in citrate buffer, incubation with primary (phosphoSer465/467-Smad2 or Smad4) and biotynilated secondary antibodies, and a short incubation with Nova-Red. The sections were counter stained with hematoxylin.

Western blot analysis
Cells were harvested as described previously (48). Primary antibody incubation was performed overnight at 4 ºC using AnxA1, AnxA2, Smad4, phosphoSer465/467-Smad2, Smad2 or tubulin antibody. Thereafter blots were incubated with horseradish peroxidase conjugated secondary antibody (GE Healthcare) in TBS-T for 1h at room temperature. Protein signals were detected with ECL-plus method (GE Healthcare) followed by scanning of the blots with a Typhoon 9400 (GE Healthcare).

Luciferase assays. Cells cultured in 48 wells plates were transfected with $(CAGA)_{12}$-transcriptional luciferase (38) and renilla reporter constructs using Lipofectamine Plus reagent (Invitrogen). The following day cells were serum starved and exposed to TGFβ1 (24 hours) thereafter cells were lysed and luciferase-activity was measured using the dual-luciferase reporter assay system (Promega).

Patient selection and study design. Schmidt et al. conducted a retrospective cohort study of breast cancer patients (39). This cohort includes women who received surgery for invasive breast cancer in Leiden University Medical Center [LUMC, Leiden, the Netherlands], and two regional hospitals in Leiden between 1970 and 1995 (40). The study received approval of the Medical Ethical Committee of the Leiden University Medical Center. The tissue micro array (TMA) represented 518 cases of breast carcinoma; 66 cases were not analyzed for technical reasons.

Tissue micro array (TMA). Tumor characteristics were all derived from a review of slides stained with hematoxylin and eosin (HE) and from TMAs including three punches per tumor. Tumor grading, according to the Bloom-Richardson method (41) and tumor morphology typing was performed as described previously (39). Immunohistochemical staining of the tissue arrays for AnxA1 was performed at the Pathology Department of the LUMC according to the protocol described in Baelde et al. (42). Evaluation of AnxA1, AnxA2, Src, CK5 and CK8 expression levels was performed independently by two scientists and a pathologist (MvM, MdG, V.S.). The intensity of the staining was scored on a 0 to 3 scale. Evaluation of ER, PR, p53, and Her2 was performed as described previously (39). Only those breast carcinomas where staining for all the 8 immunohistochemical markers was successful (n=295) were included for hierarchical unsupervised cluster analysis

(UPGMA method; assuming Euclidian distances between scores) using the GEPAS package.

Statistical analysis in vitro and in vivo. Tissue microarray statistical analysis was done using Statistical Package for the Social Sciences SPSS 15.0 (SPSS, inc.) and differences in proportions were tested by Pearson Chi-Square. For *in vitro* and *in vivo* animal studies, Student's t-test was used to determine if there was a significant difference between two means ($p<0.05$). When multiple means were compared, significance was determined by one-way analysis of variance (ANOVA; $p<0.05$). Significant differences are marked in the graphs.

Acknowledgments
We thank Gabri van de Pluijm for his suggestions, Martine van Duijn for help with the experiments, Hans de Bont for his help with the imaging, Erik Danen and Leo Price for critically reading the manuscript, Renate de Groot (NKI-AVL) for the construction of the TMAs, and the members of the Division of Toxicology of the Leiden/Amsterdam Center for Drug Research for valuable discussion and support. We are grateful to Dr. V. Gerke (University of Munster, Germany) for AnxA1 expression constructs. This work was supported by grants from the Dutch Cancer Society (KWF) (grant UL 2006-3538 and UL 2007-3860), EU FP7-Metafight (grant nr. 201862), TI Pharma project T3-107, the Dutch Organization for Scientific Research (NWO 911-02-022), and Centre for Biomedical Genetics.

Reference List

1. Lim, L. H. & Pervaiz, S. (2007) Annexin 1: the new face of an old molecule. *FASEB J.* **21**, 968-975.
2. de Graauw, M., Tijdens, I., Smeets, M. B., Hensbergen, P. J., Deelder, A. M. & van de Water B. (2008) Annexin A2 phosphorylation mediates cell scattering and branching morphogenesis via cofilin Activation. *Mol. Cell Biol.* **28**, 1029-1040.
3. Fidler, I. J. (2003) The pathogenesis of cancer metastasis: the 'seed and soil' hypothesis revisited. *Nat. Rev. Cancer* **3**, 453-458.
4. Ahn, S. H., Sawada, H., Ro, J. Y. & Nicolson, G. L. (1997) Differential expression of annexin I in human mammary ductal epithelial cells in normal and benign and malignant breast tissues. *Clin. Exp. Metastasis* **15**, 151-156.
5. Bai, X. F. et al. (2004) Overexpression of annexin 1 in pancreatic cancer and its clinical significance. *World J. Gastroenterol.* **10**, 1466-1470.
6. Garcia Pedrero, J. M. et al. (2004) Annexin A1 down-regulation in head and neck cancer is associated with epithelial differentiation status. *Am. J. Pathol.* **164**, 73-79.
7. Sorlie, T. et al. (2001) Gene expression patterns of breast carcinomas distinguish tumor subclasses with clinical implications. *Proc. Natl. Acad. Sci. U. S. A* **98**, 10869-10874.
8. Sorlie, T. et al. (2003) Repeated observation of breast tumor subtypes in independent gene expression data sets. *Proc. Natl. Acad. Sci. U. S. A* **100**, 8418-8423.
9. Rouzier, R. et al. (2005) Breast cancer molecular subtypes respond differently to preoperative chemotherapy. *Clin. Cancer Res.* **11**, 5678-5685.
10. Sarrio, D. et al. (2008) Epithelial-mesenchymal transition in breast cancer relates to the basal-like phenotype. *Cancer Res.* **68**, 989-997.
11. Lombaerts, M. et al. (2006) E-cadherin transcriptional downregulation by promoter methylation but not mutation is related to epithelial-to-mesenchymal transition in breast cancer cell lines. *Br. J. Cancer* **94**, 661-671.
12. Neve, R. M. et al. (2006) A collection of breast cancer cell lines for the study of functionally distinct cancer subtypes. *Cancer Cell* **10**, 515-527.
13. Blick, T. et al. (2008) Epithelial mesenchymal transition traits in human breast cancer cell lines. *Clin. Exp. Metastasis* **25**, 629-642.
14. Polyak, K. & Weinberg, R. A. (2009) Transitions between epithelial and mesenchymal states: acquisition of malignant and stem cell traits. *Nat. Rev. Cancer* **9**, 265-273.
15. Laping, N. J. et al. (2002) Inhibition of transforming growth factor (TGF)-beta1-induced extracellular matrix with a novel inhibitor of the TGF-beta type I receptor kinase activity: SB-431542. *Mol. Pharmacol.* **62**, 58-64.
16. Lelekakis, M. et al. (1999) A novel orthotopic model of breast cancer metastasis to bone. *Clin. Exp. Metastasis* **17**, 163-170.
17. Nielsen, T. O. et al. (2004) Immunohistochemical and clinical characterization of the basal-like subtype of invasive breast carcinoma. *Clin. Cancer Res.* **10**, 5367-5374.
18. Rakha, E. A. et al. (2007) Breast carcinoma with basal differentiation: a proposal for pathology definition based on basal cytokeratin expression. *Histopathology* **50**, 434-438.

19. van de Vijver, M. J. et al. (2002) A gene-expression signature as a predictor of survival in breast cancer. *N. Engl. J. Med.* **347**, 1999-2009.
20. Deckers, M. et al. (2006) The tumor suppressor Smad4 is required for transforming growth factor beta-induced epithelial to mesenchymal transition and bone metastasis of breast cancer cells. *Cancer Res.* **66**, 2202-2209.
21. Padua, D. et al. (2008) TGFbeta primes breast tumors for lung metastasis seeding through angiopoietin-like 4. *Cell* **133**, 66-77.
22. Tan, A. R., Alexe, G. & Reiss, M. (2008) Transforming growth factor-beta signaling: emerging stem cell target in metastatic breast cancer? *Breast Cancer Res. Treat.*
23. Futter, C. E. & White, I. J. (2007) Annexins and endocytosis. *Traffic.* **8**, 951-958.
24. Goebeler, V., Poeter, M., Zeuschner, D., Gerke, V. & Rescher, U. (2008) Annexin A8 regulates late endosome organization and function. *Mol. Biol. Cell* **19**, 5267-5278.
25. Morel, E. & Gruenberg, J. (2007) The p11/S100A10 light chain of annexin A2 is dispensable for annexin A2 association to endosomes and functions in endosomal transport. *PLoS. ONE.* **2**, e1118.
26. Morel, E. & Gruenberg, J. (2009) Annexin A2 binding to endosomes and functions in endosomal transport are regulated by tyrosine 23 phosphorylation. *J. Biol. Chem.* **284**, 1604-1611.
27. Morel, E., Parton, R. G. & Gruenberg, J. (2009) Annexin A2-dependent polymerization of actin mediates endosome biogenesis. *Dev. Cell* **16**, 445-457.
28. Seemann, J., Weber, K., Osborn, M., Parton, R. G. & Gerke, V. (1996) The association of annexin I with early endosomes is regulated by Ca2+ and requires an intact N-terminal domain. *Mol. Biol. Cell* **7**, 1359-1374.
29. Chen, Y. G. (2009) Endocytic regulation of TGF-beta signaling. *Cell Res.* **19**, 58-70.
30. Hayes, S., Chawla, A. & Corvera, S. (2002) TGF beta receptor internalization into EEA1-enriched early endosomes: role in signaling to Smad2. *J. Cell Biol.* **158**, 1239-1249.
31. Penheiter, S. G. et al. (2002) Internalization-dependent and -independent requirements for transforming growth factor beta receptor signaling via the Smad pathway. *Mol. Cell Biol.* **22**, 4750-4759.
32. Hayes, M. J., Rescher, U., Gerke, V. & Moss, S. E. (2004) Annexin-actin interactions. *Traffic.* **5**, 571-576.
33. Nagle, R. B. et al. (1986) Characterization of breast carcinomas by two monoclonal antibodies distinguishing myoepithelial from luminal epithelial cells. *J. Histochem. Cytochem.* **34**, 869-881.
34. Charafe-Jauffret, E. et al. (2006) Gene expression profiling of breast cell lines identifies potential new basal markers. *Oncogene* **25**, 2273-2284.
35. Neri, A., Welch, D., Kawaguchi, T. & Nicolson, G. L. (1982) Development and biologic properties of malignant cell sublines and clones of a spontaneously metastasizing rat mammary adenocarcinoma. *J. Natl. Cancer Inst.* **68** , 507-517.
36. Huigsloot, M., Tijdens, I. B., Mulder, G. J. & van de Water B. (2002) Differential regulation of doxorubicin-induced mitochondrial dysfunction and apoptosis by Bcl-2 in mammary adenocarcinoma (MTLn3) cells. *J. Biol. Chem.* **277**, 35869-35879.

37. de Graauw, M. et al. (2005) Heat shock protein 27 is the major differentially phosphorylated protein involved in renal epithelial cellular stress response and controls focal adhesion organization and apoptosis. *J. Biol. Chem.* **280**, 29885-29898.
38. Dennler, S. et al. (1998) Direct binding of Smad3 and Smad4 to critical TGF beta-inducible elements in the promoter of human plasminogen activator inhibitor-type 1 gene. *EMBO J.* **17**, 3091-3100.
39. Schmidt, M. K. et al. (2007) Breast cancer survival and tumor characteristics in premenopausal women carrying the CHEK2*1100delC germline mutation. *J. Clin. Oncol.* **25**, 64-69.
40. Schmidt, M. K., Vermeulen, E., Tollenaar, R. A. E. M., Van 't Veer, L. J. & van Leeuwen, F. E. (2009) Regulatory aspects of genetic research with residual human tissue: effective and efficient data coding. *Eur J Cancer* **45**, 2376-82.
41. Elston, C. W. & Ellis, I. O. (2002) Pathological prognostic factors in breast cancer. I. The value of histological grade in breast cancer: experience from a large study with long-term follow-up. *Histopathology* **41**, 151.
42. Baelde, H. J. et al. (2007) Reduction of VEGF-A and CTGF expression in diabetic nephropathy is associated with podocyte loss. *Kidney Int.* **71**, 637-645.

Supplemental Fig.s & tables

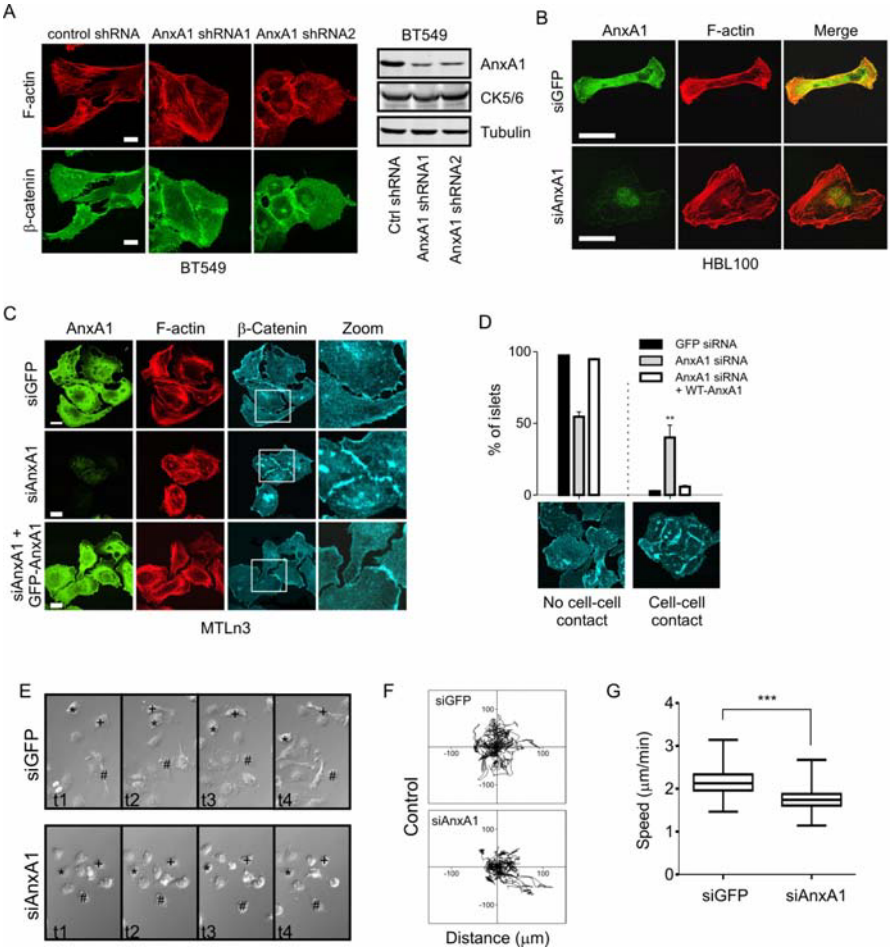

Fig. S1. *Knock-down of AnxA1 reverses the migratory phenotype of BT549 and HBL100 cells.* BT549 were transduced with lenti-viral shRNA specific for Turbo-GFP (Control shRNA) and AnxA1 (AnxA1 shRNA1). Cells were plated on collagen and subsequently fixated and stained for β-catenin (green) and F-actin (Rhodamine/phalloidin) (red). AnxA1 knock-down was quantified based on tubulin staining (A). AnxA1 knock-down was established with Dharmacon GFP siRNA (siGFP) or AnxA1 siRNA (siAnxA1) in HBL100 cells (B). Cells were stained for AnxA1 (Green) and F-actin (Rhodamine/phalloidin) (Red) and were analyzed by Confocal Laser Scanning Microscopy (A-B). Bars, 20 μm. Knockdown in MTLn3 cells was established with Dharmacon GFP siRNA (siGFP) or AnxA1 siRNA (siAnxA1) (C-D). GFP-AnxA1 was re-expressed using lipofectamine plus as described

in materials and methods (C, lower panel). Cells were stained for AnxA1 (Green), F-actin (Rhodamine/phalloidin) (Red) and β-Catenin (Blue) and analyzed by Confocal Laser Scanning Microscopy (D). The percentage of islets that formed cell-cell interactions were quantified, ** $p<0.01$ compared to control. Migration of MTLn3 cells was visualized (n = 8 movies with approx. 25 cells/movie) and time frames were extracted from the movies of cells with an interval of 30 minutes. Cell migration is indicated for 3 cells (indicated with $^{\#}$, * and $^{+}$) (E). Direction and distance of migration was determined by plotting the cell paths (F). Migration speed is indicated by Box-Whisker plot, *** $p<0.001$ (G).

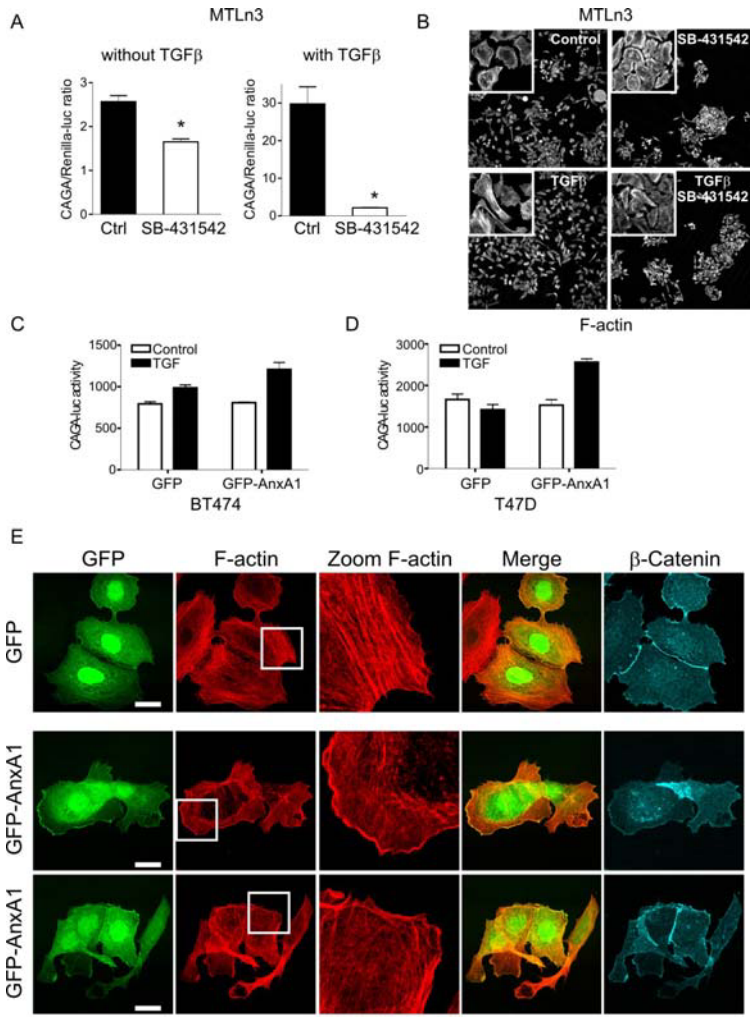

Fig. S2. *TGFβ induced $(CAGA)_{12}$-Luciferase activity and morphological changes.* MTLn3 cells were transiently transfected with $(CAGA)_{12}$-luciferase and thereafter treated with TGFβ (1 ng/ml) or SB-431542 (1 μM) for 24 h; note the different Y-axis in the left and right panel (A). Morphological changes induced by either TGFβ or SB-431542 were visualized by F-actin (rhodamine/phalloidin) staining (B). BT474 (C) and T47D (D) cells were transfected with GFP or GFP-AnxA1 and $(CAGA)_{12}$-luciferase and thereafter treated with TGFβ (1 ng/ml) for 24 hrs. MCF7 cells were transfected with GFP or GFP-AnxA1. Cells were plated on collagen for 24 hrs and subsequently fixated and stained for AnxA1, F-actin and β-catenin (E). Bars, 20 μm. Data are representative of three independent experiments.

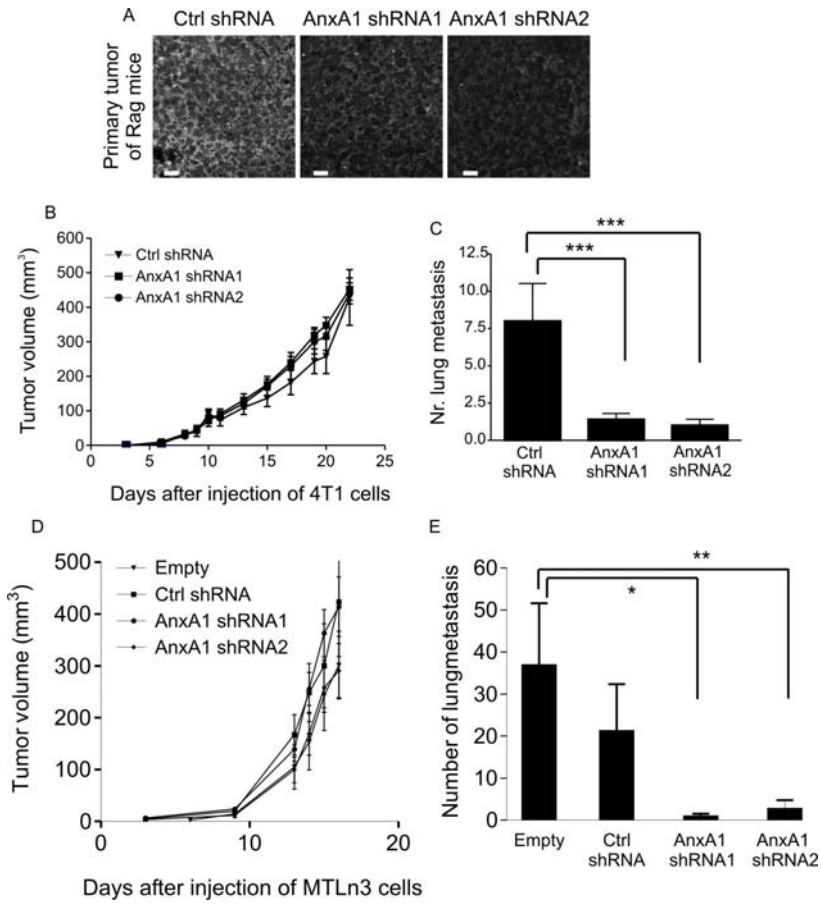

Fig. S3. *Knock-down of AnxA1 decreases the metastatic potential of highly invasive 4T1 cells.* Mouse 4T1 or rat MTLn3 breast cancer cells were transduced with lenti-viral shRNA specific for Turbo-GFP (Control shRNA) and two sequences for AnxA1 (AnxA1 shRNA1 and 2). AnxA1 shRNA1 (n=5), AnxA1 shRNA2 (n=5) and Control shRNA (n=5) 4T1 cells were injected into the mammary fat pad of 12 week old BALB/c mice. Primary tumour was evaluated for AnxA1 expression (A). Tumour volume was measured over time by callipers (B). At 24 days after injection the mice were sacrificed and lungs were isolated. Lungs were inoculated with ink as described under materials and methods and surface metastases were counted (C). MTLn3 cells were injected into the mammary fat pad of 12 week old Rag2 $^{-/-}$ /γc $^{-/-}$ mice. Tumour volume was measured over time (D) and surface metastases were counted at day 19 after injection (E).

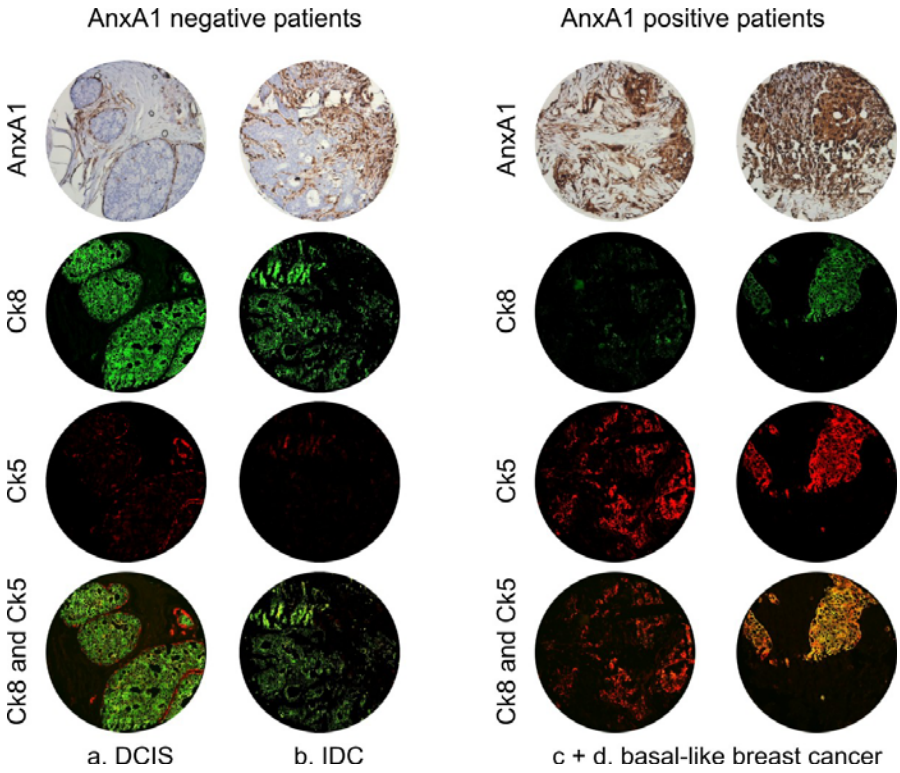

Fig. S4. *AnxA1 expression is associated with CK5 positive breast tumors*
Human breast cancer tissues (TMA of 452 patients) were stained and screened for AnxA1, CK5 and CK8 expression. Representative images for the quantification shown under Fig. 2 are shown for AnxA1 negative ductal carcinoma in situ (DCIS) (a) and invasive ductal carcinoma (IDC) (b), and for AnxA1 positive, basal-like breast cancers (c & d).

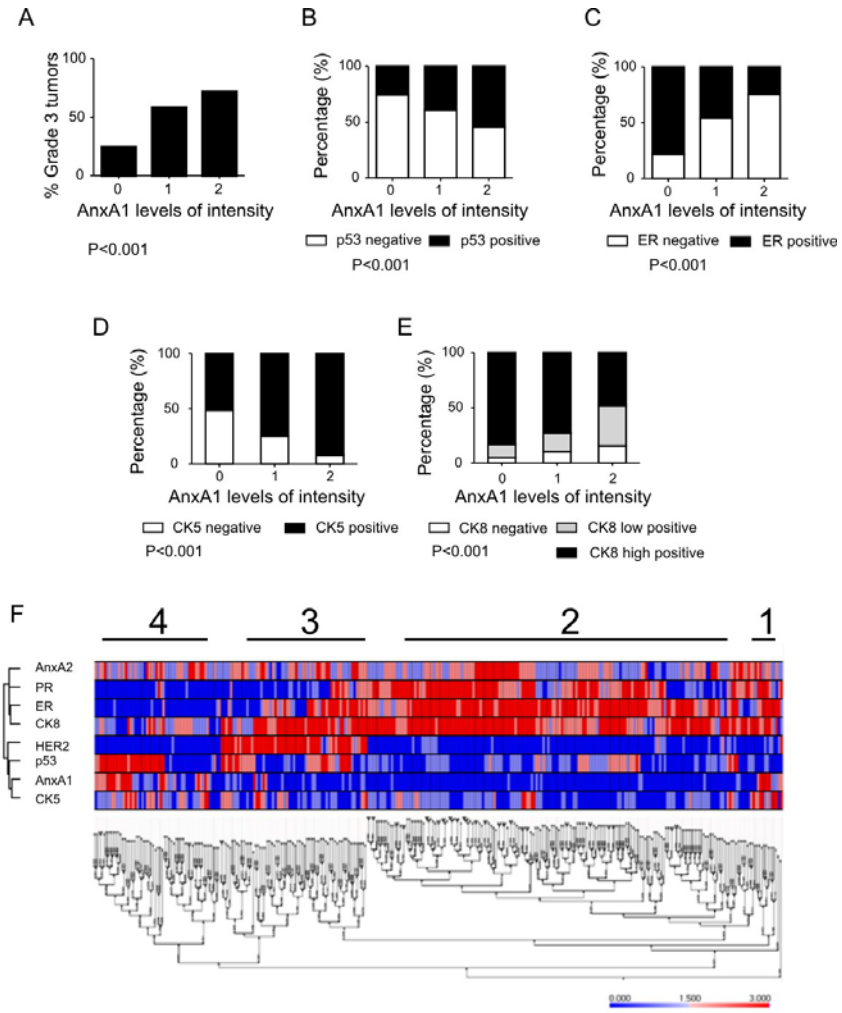

Fig. S5. *AnxA1 discriminates basal-like breast cancers from other subtypes*
Normal breast tissue was stained for AnxA1 (A). Human breast cancer tissues (TMA of 452 patients) were screened for AnxA1, AnxA2, and 6 clinical markers CK5, CK8, ER, PR, HER2 and p53. AnxA1 expression levels (0=0% tumor stained, 1= low expression, 2 = high expression) were correlated to tumor grade (A). AnxA1 expression levels (0=0% tumor stained, 1= low expression, 2 = high expression) were correlated to p53, ER, CK5 expression (0=0% tumor stained, 1=any staining) and CK8 expression (0=0% tumor stained, 1= low expression, 2 = high expression) (B-E). Only those breast carcinomas where staining for all the 8 immunohistochemical markers was successful (n=295) were included for hierarchical unsupervised cluster analysis (F) and tumors were roughly divided into four breast cancer subtypes; a small undefined CK^+/ER^+ group (1) ER^+/luminal-like (2), HER2-positive (3), and triple negative ($ER^-/PR^-/HER2^-$) (4).

Supplemental table 1
High AnxA1 expression correlates with high tumour grade, high p53, low ER, high CK5 and low CK8 expression. Human breast cancer tissues were analyzed for a correlation between AnxA1 levels and tumour grade, p53, ER, basal cell marker CK5 and luminal epithelial marker CK8. AnxA1 expression levels (0=0% tumor stained, 1= low expression, 2 = high expression) were correlated to tumor grade (Table 1A), p53 (Table 1B), ER (Table 1C), CK5 expression (0=0% tumor stained, 1=any staining) (Table 1D) and CK8 expression (0=0% tumor stained, 1= low expression, 2 = high expression) (Table 1E).

Table 1A AnxA1 expression versus tumor grade P <0.001

Expression			grade			Total
			1.00	2.00	3.00	1.00
AnxA1	0	Count	117	110	73	300
		% within grade	84.2%	84.0%	48.7%	71.4%
	1	Count	16	12	39	67
		% within grade	11.5%	9.2%	26.0%	16.0%
	2	Count	6	9	38	53
		% within grade	4.3%	6.9%	25.4%	12.6%
Total		Count	139	131	150	420
		% within grade	100.0%	100.0%	100.0%	100.0%

Table 1B AnxA1 expression versus mutant p53 expression P <0.001

Expression			P53		Total
			.00	1.00	.00
AnxA1	0	Count	208	71	279
		% within P53	77.6%	58.7%	71.7%
	1	Count	39	25	64
		% within P53	14.6%	20.7%	16.5%
	2	Count	21	25	46
		% within P53	7.8%	20.7%	11.8%
Total		Count	268	121	389
		% within P53	100.0%	100.0%	100.0%

Table 1C AnxA1 expression versus ER expression P <0.001

Expression			ER		Total
			.00	1.00	.00
AnxA1	0	Count	65	232	297
		% within ER	48.1%	85.3%	73.0%
	1	Count	33	28	61
		% within ER	24.4%	10.3%	15.0%
	2	Count	37	12	49
		% within ER	27.4%	4.4%	12%
Total		Count	135	272	407
		% within ER	100.0%	100.0%	100.0%

Table 1D AnxA1 expression versus CK5 expression P <0.001

Expression			CK5/6 expression		Total
			0	1	
AnxA1	0	Count	131	139	270
		% within AnxA1	48.5%	51.5%	100.0%
	1	Count	13	39	52
		% within AnxA1	25.0%	75%	100.0%
	2	Count	4	46	50
		% within AnxA1	8.0%	92.0%	100.0%
Total		Count	243	148	143
		% within AnxA1	88.7%	39.8%	38.4%

Table 1E AnxA1 expression versus CK8 expression P <0.001

Expression			CK8 expression			Total
			0	1	2	
AnxA1	0	Count	14	35	245	294
		% within AnxA1	4.8%	11.9%	83.3%	100.0%
	1	Count	6	10	43	59
		% within AnxA1	10.2%	16.9%	72.9%	100.0%
	2	Count	8	19	25	52
		% within AnxA1	15.4%	36.5%	48.1%	100.0%
Total		Count	28	64	313	405
		% within AnxA1	6.9%	15.8%	77.3%	100.0%

Supplemental table 2
AnxA1 expression correlates with basal-like subtype. AnxA1 RNA expression was analysed in the poor prognosis profile of van 't Veer *et al*. [19] and correlated with 5 breast cancer subtypes (e.g. basal-like, HER2$^+$, luminal A, luminal B, normal.

AnxA1

	N	Mean	Std. Dev.	Std. Error	95% Confidence Interval for Mean Lower Bound	95% Confidence Interval for Mean Upper bound	Min.	Max.
Basal	46	.10963	.272274	.040145	.02878	.19049	-.666	.816
Her2	49	-.00298	.242618	.034660	-.07267	.06671	-.624	.500
Luminal A	88	-.13567	.216477	.023077	-.18154	-.08980	-.588	.380
Luminal B	81	-.10578	.198169	.022019	-.14960	-.06196	-.614	.326
Normal	31	-.01481	.210098	.037735	-.09187	.06226	-.358	.544
Total	295	-.05447	.239864	.013965	-.08196	-.02699	-.666	.816

P<0.001

Basal-like versus other subtypes (LSD posthoc test: basal versus HER2, p=0.015, basal versus LumA p=<0.001, basal versus LumB p<0.001, basal versus normal p=0.018)